J. Phys. Chem. A **1997,** *101,* 3449−3453

Nonequilibrium Molecular Dynamics Simulations of 3-Methylhexane: The Effect of Inter- and Intramolecular Potential Models on Simulated Viscosity

Maija Lahtela* and Tapani A. Pakkanen

Department of Chemistry, University of Joensuu, P.O. Box 111, FIN-80101 Joensuu, Finland

Richard L. Rowley

Brigham Young University, Provo, Utah 84602

Received: November 25, 1996; In Final Form: March 5, 1997[⊗]

Nonequilibrium molecular dynamics simulations of viscosity were performed using various molecular representations of 3-methylhexane in order to study the influence of potential models on simulated viscosity. The models investigated were united atom models with fixed bond lengths and bond angles. The effect of intermolecular potential was examined by comparing results from a homogeneous (in which all $-CH_x$ groups are equivalent) model and two heterogeneous models. The effect of intramolecular potential was investigated by comparing results from three different torsional potential models. The simulations were carried out at three different densities to investigate the sensitivity of the contributions from the various models to the viscosity at different conditions. Large changes in viscosity were produced by relatively small changes in the intermolecular potential parameters of the branched methyl group. The viscosity was found to be less sensitive to the intermolecular potential parameters of the chain methyl groups and the torsional potential. Our results suggest that an accurate representation of the molecular structure and size as governed by intermolecular interactions is more important in accurate viscosity predictions than careful modeling of the intramolecular potential.

I. Introduction

There is growing interest in understanding the liquid-state behavior of linear and branched alkanes of moderate size (C_4−C_{40}). For example, the ability to accurately determine fluid viscosity from molecular structure and knowledge of the inter- and intramolecular interactions is a problem of practical importance in lubricant design. The increasing power and availability of computational facilities have made molecular simulations an intriguing and useful method for investigation of fluid properties on a molecular scale.

Nonequilibrium molecular dynamics (NEMD)[1−3] simulations of Couette flow have been used extensively to obtain viscosities of model *n*-alkanes.[4−23] Generally, viscosities obtained from such simulations are in reasonably good agreement with experimental values.[6−10] However, only recently has the viscosity of branched alkanes been studied by molecular simulations.[9,16,20] As far as we know, NEMD simulations of branched alkanes have only been reported for isobutane, 5-butylnonane, and squalane.[9,16,20] While it is assumed that the description of both inter- and intramolecular forces must be accurately handled to produce accurate viscosities, it is of value for future model development to identify the sensitivity of the predictions to various portions of the model. In this work, we simulate the viscosity of 3-methylhexane using three different intramolecular potentials and three different sets of Lennard-Jones (LJ) parameters for the various interacting sites. To focus explicitly on these issues, we restrict this study to united atom (UA) models in which hydrogen atoms are not explicitly modeled and to models of fixed bond length and angle. However, the dihedral angles in the molecule are allowed to change in accordance with a prescribed intramolecular potential. While some simulations have been reported in which angle bending and/or bond vibrations are allowed,[22,23] the extremely small time step required makes such methods inefficient, especially since results thus far have not compared favorably with experimental values. Indeed, a recent study showed that for equilibrium properties the inclusion of flexibility in a rigid model "does not improve quality and runs the risk of producing worse artifacts than are inherent in rigid models.[24]" There is hope that methods for accurately simulating viscosity can be achieved with coarser, more efficient models, if the weak links in these current models can be identified, and this is the focus of this paper.

The purpose of this work is to examine the efficacy of using intermolecular parameters regressed from *n*-alkane simulations to simulate viscosities for branched alkanes and the relative importance of the intermolecular potential model for the branched molecule in obtaining accurate viscosities. Ultimately we hope to identify appropriate models and parameters that can be used to accurately and quantitatively simulate the viscosity of even quite complex fluids that may be important as commercial lubricants. However, we start with a small branched alkane to more clearly identify the effects.

II. The Model

Several types of intermolecular potential models have been proposed for *n*-alkanes.[25−27] The most commonly used is a simple site−site UA model in which the methyl, methylene, and methine groups are represented by a single, spherically symmetric interaction site located at the carbon nuclei. The advantage of the UA model is its computational simplicity while still correctly modeling the skeletal structure. The homogenous UA model[9,10,15] treats equivalently all methyl, methylene, and methine groups by using the same interaction parameters regardless of the number of attached hydrogen atoms. The LJ parameters for this model were calculated by Ryckaert and Bellemans[28] by adjusting σ and ϵ for *n*-butane. The model has

---

[⊗] Abstract published in *Advance ACS Abstracts,* April 15, 1997.

TABLE 1: Model Parameters

model	parameter	value
homogenous UA	m	2.411×10^{-26} kg
	ϵ/k	72.0 K
	σ	0.3923 nm
OPLS (heterogeneous) UA	$m(CH_3)$	2.4966×10^{-26} kg
	$m(CH_2)$	2.385×10^{-26} kg
	$m(CH)$	2.1619×10^{-26} kg
	$\epsilon/k(CH_3)$	88.067 K
	$\epsilon/k(CH_2)$	59.386 K
	$\epsilon/k(CH)$	40.581 K
	$\sigma(CH_3)$	0.3923 nm
	$\sigma(CH_2)$	0.3905 nm
	$\sigma(CH)$	0.3850 nm
adjusted branched parameter	σ(branched $-CH_3$)	0.5125 nm

been shown to accurately predict the viscosity of small alkanes,[9,15] but tends to underpredict viscosities of larger molecules. The heterogeneous UA model uses intermolecular interaction parameters that are unique for each $-CH_x$ group. We use here the OPLS model parameters optimized by Jorgensen et al.[27]

We have used both the homogenous and heterogenous UA models for 3-methylhexane to see the effect of small changes in intermolecular interactions. Table 1 summarizes the model parameters used. Interactions between sites of different molecules were modeled with the LJ potentials. The Lorentz–Berthelot combining rule was used for all cross interactions. We also varied σ for the branched $-CH_3$ group to estimate the sensitivity of the viscosity to the lone branched group.

Three different potential models were used to model internal rotations about torsional angles. In the rigid model, we constrained all torsional angles to their *trans* configurations. Flexibility was introduced into the molecule by allowing all three dihedral angles to move in accordance with the Ryckaert–Bellemans[28] (RB) intramolecular potential function,

$$\Phi_{\mathrm{dihedral}}(\phi)/k = \sum_{i=0}^{5} a_i \cos^i(\phi) \qquad (1)$$

that has been developed for *n*-alkanes. In eq 1, U is potential energy, k is Boltzmann's constant, ϕ is the dihedral angle, and a_i are expansion coefficients. The RB potential model also includes internal LJ interactions between sites separated by more than four carbons. Simulations have also been reported that have used a torsional potential function developed by Steele from *ab initio* calculations for *n*-butane.[29] Stindham and During,[30] Toxvaerd et al.,[31,32] and Raghavachari[33] have also proposed different torsional potential functions for *n*-alkane fluid models. In general, the torsional potential is presented as a series of cosine functions similar to the RB potential, but the number of terms and the coefficients vary.

For the third intramolecular potential model, the RB potential was used for the torsional angle not involving the side chain, but a more accurate potential was developed for the two torsional angles involving the branched methyl group. This is similar to the procedure used by Mondello and Grest.[20] Mondello and Grest's potential function is similar to eq 1 except there are two series for different dihedral angles, one for $X-CH_2-CH_2-Y$ and the other for $X-CH_2-CH(CH_3)-Y$, where X and Y can be either a methyl or methylene group. We have regressed parameters in the equation

$$U(\phi) = a_1 + a_2\cos(3\phi) + a_3x + a_4x^2 + a_5x^4 + a_6x^5 \qquad (2)$$

for the two torsional angles involving the side methyl group from energies computed using Hyperchem. In eq 2 $x = \cos^{-1}(\phi)$. Values of the parameters are given in Table 2, and the potential as a function of dihedral angle is shown in Figure 1.

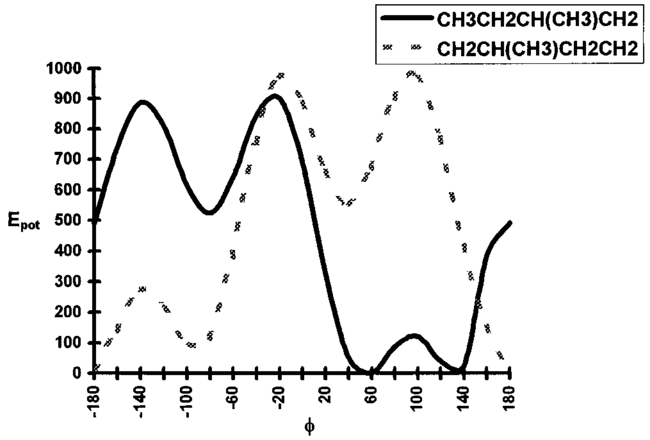

Figure 1. Intramolecular potential from eq 2 as a function of dihedral angle for the $CH_3-CH_2-CH(CH_3)-CH_2$ and $CH_2-CH(CH_3)-CH_2-CH_2$ torsional groups.

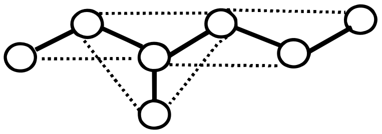

Figure 2. UA model for 3-methylhexane showing the bond length constraints (solid lines) and the bond angle constraints (broken lines).

TABLE 2: Coefficients for eq 1 and eq 2

	eq 1	eq 2 $CH_3-CH_2-CH(CH_3)-CH_2$	eq 2 $CH_2-CH(CH_3)-CH_2-CH_2$
a_1	1116	671.441	705.827
a_2	1462	228.635	212.350
a_3	−1578	229.265	258.293
a_4	−368	−157.065	−119.939
a_5	3156	15.224	9.407
a_6	−3788	2.382	−2.243

III. Simulation Details

All NEMD simulations were performed using an NVT algorithm developed by Edberg et al.[7] The code used a molecular version of the SLLOD (isothermal shear) algorithm.[34,35] Gauss's principle of least constraints was used to evaluate the constraint forces for the bond, angle, and thermostat constraints.[3,26,34] Figure 2 shows the geometry of the seven connected sites, illustrating the nearest neighbor and next-nearest-neighbor distance constraints that were used to fix the bond distances and bond angles. The simulated system was composed of 216 molecules in a cubic cell with periodic boundary conditions. The LJ site potential was truncated at $r = 2.5\sigma$, and standard long-range potential cutoff corrections were included. A Gaussian constraint was also imposed to homogeneously force the molecules to move with a linear velocity profile in one direction, thereby modeling Couette flow. Details of the simulation code are available elsewhere.[9,10,15]

The simulations were performed at conditions corresponding to those for which experimental data were available. Three state points were examined: (1) $T = 350$ K, $\rho_g = 574.781$ kg·m^{-3}; (2) $T = 300$ K, $\rho_g = 613.632$ kg·m^{-3}; and (3) $T = 250$ K, $\rho_g = 644.827$ kg·m^{-3}. The simulations were carried out at several shear rates in the range 3.5×10^{-10} s^{-1} $\leq \gamma \leq 14.1 \times 10^{-10}$ s^{-1} in order to ascertain the dependence of simulated viscosity on shear rate and in order to extrapolate the viscosity to $\gamma = 0$ for comparison with the experimental value.

TABLE 3: Viscosities (in 10^{-4} Pa·s) of 3-Methylhexane for Different Models at 350 K

intermolec model	intramolec model	$\gamma = 140$ ns^{-1} (Stdev)	$\gamma = 90$ ns^{-1} (Stdev)	$\gamma = 69$ ns^{-1} (Stdev)	$\gamma = 51$ ns^{-1} (Stdev)	$\gamma = 35$ ns^{-1} (Stdev)	$\gamma = 0$
homogeneous	rigid	1.083	1.112	1.121	1.174		1.201
		(0.14)	(0.25)	(0.21)	(0.12)		
homogeneous	eq 1	1.183	1.212	1.222	1.311		1.336
		(0.09)	(0.14)	(0.03)	(0.32)		
OPLS	rigid	1.040	1.018	1.045	1.001		1.007
		(0.07)	(0.08)	(0.10)	(0.32)		
OPLS	eq 1	1.134	1.172	1.168	1.201	1.193[a]	1.287
		(0.11)	(0.13)	(0.37)	(0.41)	(0.42)	
OPLS	eq 2	1.153	1.211	1.216	1.200	1.293	1.375
		(0.07)	(0.14)	(0.09)	(0.22)	(0.21)	
OPLS/ (adj σ_{branched})	eq 2	1.767	1.806	1.851	2.009		2.060
		(0.13)	(0.15)	(0.13)	(0.14)		

[a] Value not used in extrapolation to zero shear.

TABLE 4: Viscosities (in 10^{-4} Pa·s) of 3-Methylhexane for Different Models at 300 K

intermolec model	intramolec model	$\gamma = 140$ ns^{-1} (Stdev)	$\gamma = 90$ ns^{-1} (Stdev)	$\gamma = 69$ ns^{-1} (Stdev)	$\gamma = 51$ ns^{-1} (Stdev)	$\gamma = 35$ ns^{-1} (Stdev)	$\gamma = 0$
homogeneous	rigid	1.375	1.506	1.520	1.550		1.659
		(0.17)	(0.22)	(0.11)	(0.24)		
homogeneous	eq 1	1.535	1.645	1.517	1.576		1.586
		(0.08)	(0.08)	(0.35)	(0.07)		
OPLS	rigid	1.259	1.265	1.346	1.412		1.460
		(0.12)	(0.20)	(0.14)	(0.02)		
OPLS	eq 1	1.316	1.366	1.393	1.557	1.481[a]	1.821
		(0.07)	(0.05)	(0.41)	(0.62)	(0.16)	
OPLS	eq 2	1.474	1.495	1.525	1.555	1.494[a]	1.667
		(0.04)	(0.11)	(0.20)	(0.33)	(0.35)	
OPLS (adj σ_{branched})	eq 2	2.483	2.694	2.713	2.763		3.201
		(0.07)	(0.24)	(0.27)	(0.37)		

[a] Value not used in extrapolation to zero shear.

TABLE 5: Simulated Viscosities (in 10^{-4} Pa·s) for 3-Methylhexane for Different Models at 250 K

intermolec model	intramolec model	$\gamma = 140$ ns^{-1} (Stdev)	$\gamma = 90$ ns^{-1} (Stdev)	$\gamma = 69$ ns^{-1} (Stdev)	$\gamma = 51$ ns^{-1} (Stdev)	$\gamma = 35$ ns^{-1} (Stdev)	$\gamma = 0$
homogeneous	rigid	1.857	2.081	2.170	2.237		2.570
		(0.12)	(0.07)	(0.11)	(0.10)		
homogeneous	eq 1	1.969	2.050	2.140	2.272		2.382
		(0.27)	(0.13)	(0.29)	(0.28)		
OPLS	rigid	1.515	1.652	1.746	1.751		1.911
		(0.15)	(0.05)	(0.24)	(0.02)		
OPLS	eq 1	1.807	1.900	2.007	1.958	1.921[a]	2.188
		(0.16)	(0.10)	(0.07)	(0.22)	(0.30)	
OPLS	eq 2	1.698	1.770	1.860	1.969	2.010	2.342
		(0.03)	(0.07)	(0.20)	(0.46)	(0.50)	
OPLS (adj σ_{branched})	eq 2	3.376	3.529	3.858	4.108		4.503
		(0.32)	(0.33)	(0.79)	(0.17)		

[a] Value not used in extrapolation to zero shear.

Simulations were initiated from a crystal lattice. A fifth-order predictor corrector method was used to perform the integration using a step size of 2.9 fs. Fifty time steps were used to melt the crystal lattice, 50 000 time steps were used to equilibrate the fluid under Couette flow, and four block averages of 50 000 time steps each, or 200 000 total time steps, were used for the production runs. A multiple time step algorithm previously developed and tested for viscosity simulations was used to enhance the efficiency of the simulation.[15] The viscosity was obtained as a time average of the *xy* and *yx* elements of the pressure tensor corresponding to the Couette flow geometry.

IV. Results and Discussion

The results of our simulations are shown in Tables 3, 4, and 5. Shear thinning was observed over the entire shear range, consistent with previous studies of model alkanes.[9,15,16] The viscosity at zero shear, $\eta(0)$, was obtained from a linear least-squares fit of the simulated $\eta(\gamma)$ values using the equation $\eta(\gamma) = \eta(0) - A\gamma^{1/2}$.[13] This is the commonly accepted method for extrapolation to zero shear. Recently some have suggested that a plateau exits at very short shear rates if η is plotted versus γ. However, special procedures and very long simulations must be performed in order to reduce the noise-to-signal ratio in this region sufficiently that the plateau region can be observed with any reliability. Our experience has been that extrapolation against $\gamma^{1/2}$ gives values that are in good agreement with equilibrium molecular dynamics simulations (EMD) and that are within the uncertainty of the values obtained from the plateau method. It is also well-known that NVT simulations at high shear rates deviate from linearity with $\gamma^{1/2}$. All of our extrapolations were performed over the moderate shear rate for which Daivis and Evans[18] have shown that NVT and NPT ensembles produce identical results. Figures 3−5 show that the linear extrapolation with respect to $\gamma^{1/2}$ is valid over the range of shear rates used in the simulation. As additional confirmation of the validity of this procedure, equilibrium

TABLE 6: Comparison of Simulated and Experimental Viscosities (in 10^{-4} Pa·s) for 3-Methylhexane

T/(K)	homg/rigid	homg/eq 1	EMD homg/eq 1	OPLS/rigid	OPLS/eq 1	EMD OPLS/eq 1	OPLS/eq 2	OPLS-adj σ_{branch}/eq 2	exptl[37]
350	1.201	1.336	1.085	1.007	1.287	1.493	1.375	2.060	2.119
300	1.659	1.586	1.839	1.460	1.821	1.871	1.667	3.201	3.393
250	2.570	2.382	2.027	1.911	2.188	2.854	2.342	4.503	6.553

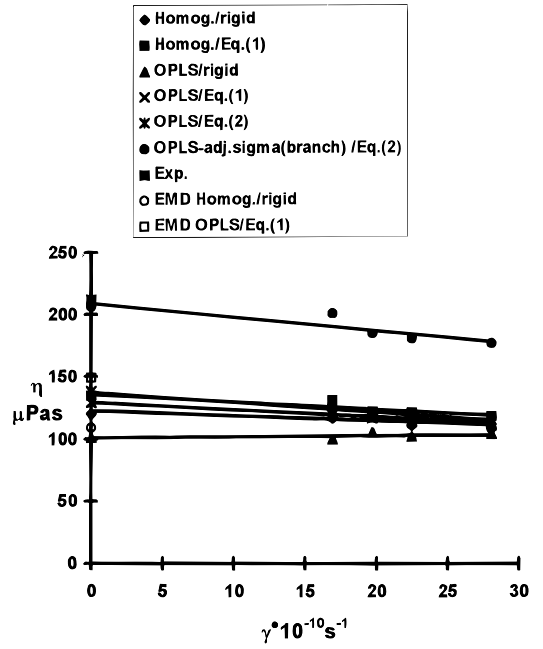

Figure 3. Linear extrapolation of $\eta(\gamma)$ values obtained from the different models to $\gamma = 0$ and at 350 K and comparison to the EMD value (open symbols) for OPLS/rigid and OPLS/eq 1 models.

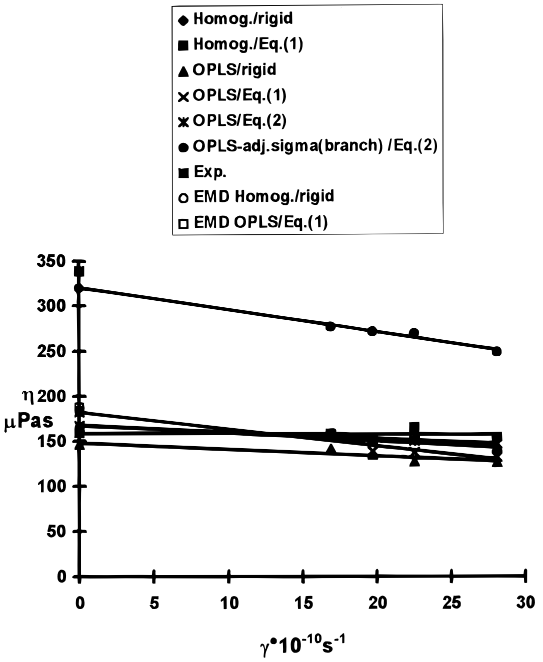

Figure 4. Linear extrapolation of $\eta(\gamma)$ values obtained from the different models to $\gamma = 0$ and at 300 K and comparison to the EMD value (open symbols) for OPLS/rigid and OPLS/eq 1 models.

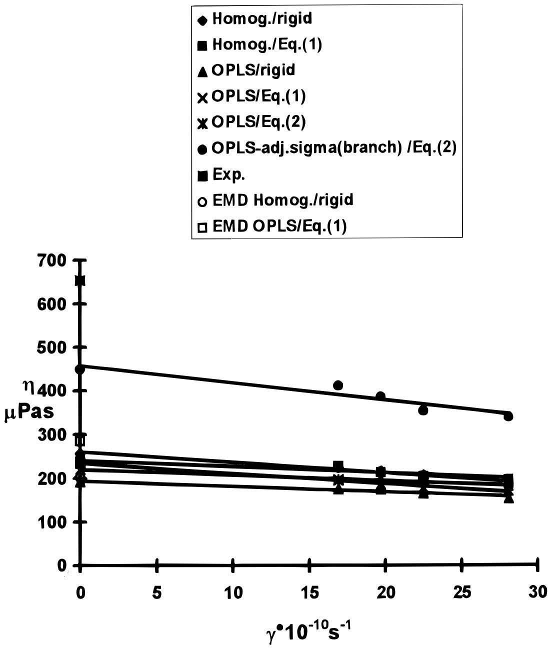

Figure 5. Linear extrapolation of $\eta(\gamma)$ values obtained from the different models to $\gamma = 0$ and at 250 K and comparison to the EMD value (open symbols) for OPLS/rigid and OPLS/eq 1 models.

molecular dynamics (EMD) simulations were also performed for the OPLS/eq 1 and OPLS/rigid models. The EMD values were calculated using multiple time origins and over 800 000 time steps. Although the uncertainty in the EMD results is larger than that for the NEMD extrapolated values, the agreement shown in Figures 3−5 between the EMD results and the extrapolated NEMD values confirms the validity of the extrapolation method used to obtain $\eta(0)$.

A comparison is made in Table 6 of the zero-shear results using the various models with the experimental values. All of the models underpredict the experimental viscosity. Our results suggest that the simulated viscosity is fairly insensitive to the internal potential. For example, there is very little difference between the values obtained using the homogeneous/rigid model and the homogeneous/eq 1 model. The flexible model produces a lower viscosity than the rigid model at higher densities (lower temperatures), but the effect is small. Interestingly, the OPLS/rigid model predictions are lower than all of the others. In the case of the OPLS intermolecular interactions, the increased flexibility about torsional angles slightly increases the simulated viscosity. There is a more significant difference between the rigid and eq 1 models for the torsional degrees of freedom than there is between the use of eq 1 and eq 2. It is apparent that improving the intramolecular potential has only a relatively small effect upon the observed viscosity and that careful fitting of the torsional potential for branched molecules is important only for very accurate predictions.

Results from the various intermolecular potential models indicate that care must be taken to get the intermolecular interactions right. Comparison of results for the homogeneous/rigid and OPLS/rigid models shows a significant decrease in the viscosity with a small change in parameter values (cf. values in Table 1). The relative change between the two rigid models becomes substantially larger with increasing density. This effect is not as obvious when comparing the homogeneous/eq 1 and OPLS/eq 1 models. A change in the size parameter of the branched methyl group (OPLS-adj $\sigma_{\mathrm{branched}}$) also produces a significant change in the simulated viscosities. As shown in

Table 6, the values predicted using this model are in relatively good agreement with experiment.

These observations suggest that simulated viscosity is more directly affected by the structure of the molecule as defined by the location of the LJ sites than by internal degrees of freedom, although the latter play an increasing important role at higher densities. Although the viscosity of *n*-alkanes can be simulated relatively well with homogeneous UA site−site interactions, predictions for this branched alkane are significantly low for all of the models investigated. We believe that detailed structure (of the branch) is more important for accurately modeling branched alkanes. Simulations have shown that *n*-alkanes tend to align with the shear field and this produces the usual shear-thinning effect.[9] However, if the molecule has a side branch, protruding segments of the molecule can not completely align with the velocity field, and they "catch" or drag as one layer moves past another. Therefore the asymmetry of sites on these side chains can have a large effect upon the viscosity. Obviously, this effect would be more significant at higher densities when molecules are more closely packed together, which is consistent with our results. The model in which we have used a larger value for σ of the branched methyl group models the extra drag from the protruding hydrogen atoms with a larger group size, and it therefore produces values for the viscosity in much closer agreement to the experimental data. In this case, a 30% increase in σ almost doubles the predicted shear viscosity.

Our results suggest that either an all-atom model, in which the hydrogen atoms are explicitly treated, or a revised UA model in which different side-chain groups are regressed from viscosity data is required to accurately model branched alkanes. The latter approach would lack information about the fine structure of the geometry that could be obtained using hydrogen sites, but it would preserve the computational efficiency obtained using UA models. We suspect that results from this modified UA model would probably still show some density dependence because of the lack of asymmetry around the carbon, but that results in reasonably good agreement with experiment could be obtained at most densities of interest.

V. Conclusions

We have performed NEMD viscosity simulations for three different intermolecular potential models and three different torisional potential models for 3-methylhexane in an effort to understand the role of the potential model on the value of the simulated viscosity. While similar models have been shown to quite accurately predict the viscosity of short-chain *n*-alkanes, all of the models for this branched molecule underpredicted significantly the actual viscosity. Accurate modeling of the torsional potential is less important than small adjustments in the LJ parameters used to model the intermolecular potential. This appears to be a structural effect. Modification of the branched methyl σ value can bring the simulated viscosities into reasonably good agreement with experimental values, suggesting that new OPLS parameters may need to be developed for branched molecules. As equilibrium properties are less sensitive to these parameters than viscosity, it would seem propitious to regress the new parameters from viscosity data in conjunction with equilibrium property data.

Acknowledgment. The financial support from Neste Ltd. is gratefully acknowledged. We would like to thank William Allen for his assistance and helpful suggestions and Norman Fuller for performing the EMD simulations.

References and Notes

(1) Evans, D. J.; Morriss, G. P. *Statistical Mechanics of Nonequilibrium Liquids*; Academic Press: London, 1990.
(2) Allen, M. P.; Tildesley, D. J. *Computer Simulation of Liquids*; Clarendon Press: Oxford, 1993.
(3) Rowley, R. L. *Statistical Mechanics for Thermophysical Property Calculations*; PTR Prentice Hall: New Jersey, 1994.
(4) Cummings, P. T.; Evans, D. J. *Ind. Eng.Chem. Res.* **1992**, *31*, 1237.
(5) Hoheisel, C. *Phys. Rep.* **1994**, *245*, 111.
(6) Maréchal, G.; Ryckaert, J-P.; Bellemans, A. *Mol. Phys.* **1987**, *61*, 33.
(7) Edberg, R.; Morriss, G. P.; Evans, D. J. *J. Chem. Phys.* **1987**, *86*, 4555.
(8) Morriss, G. P.; Evans, D. J. *Comput. Phys. Commun.* **1991**, *62*, 267.
(9) Rowley, R. L.; Ely, J. F. *Mol. Phys.* **1991**, *72*, 381.
(10) Rowley, R. L.; Ely, J. F. *Mol. Simul.* **1991**, *7*, 303.
(11) Travis, K. P.; Brown, D.; Clarke, J. H. R. *J. Chem. Phys.* **1993**, *98*, 1524.
(12) Hayashi, H.; Tanaka, H.; Nakanishi, K. *Mol. Simul.* **1993**, *9*, 401.
(13) Chynoweth, S.; Michopoulus, Y. *Mol. Phys.* **1994**, *81*, 133.
(14) Clarke, J. H. R.; Brown, D. *J. Chem. Phys.* **1987**, *86*, 1542.
(15) Rowley, R. L.; Ely, J. F. *Mol. Phys.* **1992**, *75*, 713.
(16) Daivis, P. J.; Evans, D. J.; Morriss, G. P. *J. Chem. Phys.* **1992**, *97*, 616.
(17) Padilla, P.; Toxvaerd, S. *J. Chem. Phys.* **1992**, *97*, 7687.
(18) Daivis, P. J.; Evans, D. J. *J. Chem. Phys.* **1994**, *100*, 541.
(19) Mundy, C. J.; Siepmann, J. I.; Klein, M. L. *J. Chem. Phys.* **1995**, *103*, 10192.
(20) Mondello, M.; Grest, G. P. *J. Chem. Phys.* **1995**, *103*, 7156.
(21) Morriss, G. P.; Daivis, P. J.; Evans, D. J. *J. Chem. Phys.* **1991**, *94*, 7420.
(22) Cui, S. T.; Cummings, P. T.; Cochran, H. D. *J. Chem. Phys*. **1996**, *104*, 255.
(23) Cui, S. T.; Gupta, S. A.; Cummings, P. T.; Cochran, H. D. *J. Chem. Phys*. **1996**, *105*, 1214.
(24) Tironi, I. G.; Brunne, R. M.; van Gunsteren, W. F. *Chem. Phys. Lett.* **1996**, *250,* 19.
(25) Smith, G. D.; Yoon, D. Y. *J. Chem. Phys.* **1994**, *100*, 649.
(26) Toxvaerd, S. *J. Chem. Phys.* **1990**, *93*, 4290.
(27) Jorgensen, W. L.; Madura, J. D.; Swenson, C. J. *J. Am. Chem. Soc*. **1984**, *106*, 6638.
(28) Ryckaert, J-P.; Bellemans, A. *Discuss. Faraday Soc*. **1978**, *66,* 95.
(29) Steele, D. *J. Chem. Soc., Faraday Trans. 2* **1985**, *81*, 1077.
(30) Stidham, H. D.; During, J. D. *Spectrochim. Acta Part A* **1986**, *42*, 105.
(31) Toxvaerd, S. *J. Chem. Phys.* **1988**, *89*, 3808.
(32) Toxvaerd, S.; Padilla, P. *J. Chem. Phys.* **1991**, *94*, 5650.
(33) Raghavachari, K. *J. Chem. Phys.* **1984**, *81,* 1383.
(34) Evans, D. J.; Morriss, G. P. *Phys. Rev. A* **1984**, *30*, 1528.
(35) Evans, D. J.; Morriss, G. P. *Comput. Phys. Rep*. **1984**, *1*, 297.
(36) Edberg, R.; Evans, D. J.; Morriss, G. P. *J. Chem. Phys.* **1986**, *84*, 6933.
(37) *Physical and Thermodynamic Properties of Pure Chemicals: Data Compilation*; Daubert, T. E., Danner, R. P., Eds.; Taylor and Francis: London, 1996.